

Initial performance of the magnet system in the splitter/combiner section of the Cornell-Brookhaven Energy-Recovery Linac Test Accelerator

J. A. Crittenden, J. S. Berg

June 2018

Collider Accelerator Department
Brookhaven National Laboratory

U.S. Department of Energy

USDOE Office of Science (SC), Nuclear Physics (NP) (SC-26)

Notice: This technical note has been authored by employees of Brookhaven Science Associates, LLC under Contract No. DE-SC0012704 with the U.S. Department of Energy. The publisher by accepting the technical note for publication acknowledges that the United States Government retains a non-exclusive, paid-up, irrevocable, world-wide license to publish or reproduce the published form of this technical note, or allow others to do so, for United States Government purposes.

DISCLAIMER

This report was prepared as an account of work sponsored by an agency of the United States Government. Neither the United States Government nor any agency thereof, nor any of their employees, nor any of their contractors, subcontractors, or their employees, makes any warranty, express or implied, or assumes any legal liability or responsibility for the accuracy, completeness, or any third party's use or the results of such use of any information, apparatus, product, or process disclosed, or represents that its use would not infringe privately owned rights. Reference herein to any specific commercial product, process, or service by trade name, trademark, manufacturer, or otherwise, does not necessarily constitute or imply its endorsement, recommendation, or favoring by the United States Government or any agency thereof or its contractors or subcontractors. The views and opinions of authors expressed herein do not necessarily state or reflect those of the United States Government or any agency thereof.

INITIAL PERFORMANCE OF THE MAGNET SYSTEM IN THE SPLITTER/COMBINER SECTION OF THE CORNELL-BROOKHAVEN ENERGY-RECOVERY LINAC TEST ACCELERATOR

J. A. Crittenden, A. Bartnik, R.M. Bass, D. Burke, J. Dobbins, C. Gulliford, Y. Li, D. Jusic,
D. Sagan, K. Smolenski, J. Turco
CLASSE, Cornell University, Ithaca, NY 14853, USA
J.S. Berg
Brookhaven National Laboratory, Upton, NY, USA

Abstract

The Cornell-Brookhaven Energy-recovery Linac Test Accelerator is a four-pass, 150-MeV electron accelerator with a six-cell 1.3 GHz superconducting-RF linear accelerator and a fixed-field alternating-gradient (FFAG) return loop made up of Halbach-style quadrupole magnets. The optics matching between the linear accelerator and the return loop is achieved with a conventional magnet system comprised of 50 dipole magnets and 64 quadrupole magnets in four beamlines at each end of the linac. The 42-, 78-, 114- and 150-MeV electron beams are separated into independent vacuum chambers in order to allow for the path-length adjustment required by energy recovery. We report on the first beam tests of the initial installation of the splitter/combiner section at the exit of the linac. The vacuum system of the 42-MeV S1 line was installed during the first week of April. Nine dipole and four quadrupole magnets were installed and surveyed into position the following week, and the water cooling system was commissioned. A 6-MeV beam passed through the line on April 11 with no need for adjusting pre-set magnet excitation currents. One week later, time-of-flight measurements were used to calibrate and phase the individual superconducting RF cavities. The S1 magnet settings were then scaled up to achieve 5-cavity, 42-MeV operation through the first nine FFAG permanent-magnet quadrupoles. This initial Fractional Arc Test will conclude on May 18, when the installation of the remaining seven splitter/combiner lines and the return loop will begin. CBETA operations are scheduled to begin in early 2019.

INTRODUCTION

The Cornell-Brookhaven Energy-recovery Linac Test Accelerator [1–4] is under construction at the Cornell Laboratory for Accelerator-based ScienceS and Education. When it is completed in 2019, beams will be accelerated and decelerated four times through the six-cell superconducting main linear accelerator to produce an maximum energy of 150 MeV. The four beamlines in the splitter/combiner sections at each end of the linac serve to place the beams on the design orbits through the permanent-magnet quadrupoles of the fixed-field alternating gradient (FFAG) cells in the return loop. The splitter lines also serve the purpose of adjusting path lengths to ensure energy recovery in the main linac. Following installation of the first downstream splitter line

and the first FFAG nine-magnet girder in April, 2018, a 42-MeV beam was successfully commissioned in this Fractional Arc Test (F.A.T.) We briefly describe the initial operational experience with the S1 electromagnets.

SPLITTER MAGNET DESIGN AND FABRICATION

The spatial constraints on the four splitter lines upstream and downstream of the main linac are quite severe (see Fig. 1) and dictated many aspects of the electromagnet design. The four beam momenta from the linac are initially separated by a “common magnet” (not shown here). The first magnet of the 42-MeV S1 line installed for the F.A.T. is a 5-cm-long corrector dipole. Two of the six 16-cm-long internal dipole magnets are shown. The first two of the eight quadrupoles are shown. For the F.A.T. so far, only the central four quadrupoles were available. Initial design studies

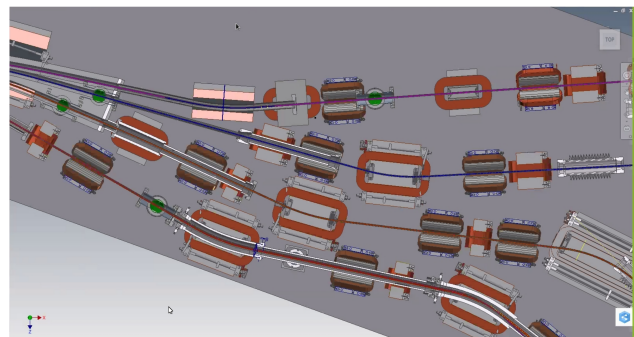


Figure 1: Schematic diagram of the upstream half of the splitter section SX downstream of the main linac. Dipole magnets are shown in gray/orange; the quadrupoles are shown in gray/blue. The areas in pink will be occupied by septum magnets.

were performed at Cornell University [5, 6]. Refinements of this design, the engineering design, and fabrication were undertaken by Elytt Energy [7]. Figure 2 shows F.A.T. S1 line magnets in place prior to the installation of the vacuum system. Note the narrowing of the dipole steel at beam height, saving crucial space for the future installation of the S2 line. The poles of these magnets are only 7.66 cm wide, but can accommodate bend angles as high as 31 degrees with a transverse uniformity of $\pm 0.05\%$ through the use of precision chamfers on the ends of the poles [6]. The first six

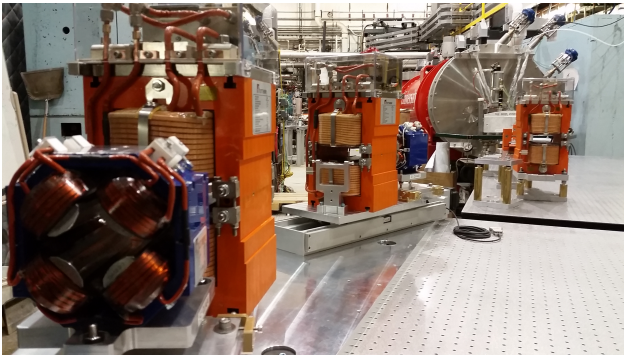


Figure 2: Two S1 quadrupoles (blue) and three S1 dipoles (orange) shown on their adjustable mounting fixtures prior to installation of the vacuum system, viewed from downstream.

dipoles, four quadrupoles and four vertical corrector magnets arrived at Cornell from Elytt/Neureus Technologies by March 26.

FRACTIONAL ARC TEST

Figures 3 and 4 show the layout of the beamline components for the F.A.T.

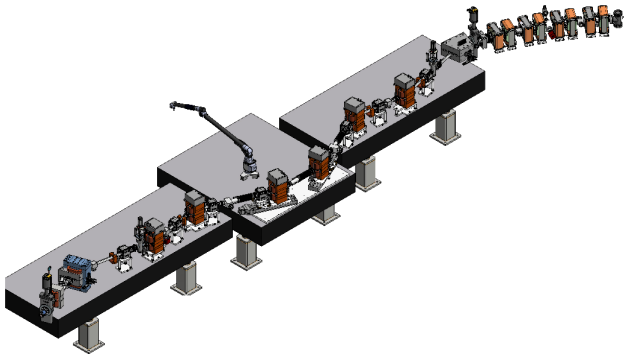


Figure 3: Splitter and FFAG cell beamline components of the Fractional Arc Test. A survey arm placement is also shown.

Table 5 shows the operating parameters at 42-MeV for the magnets in the S1 line.

Figure 6 shows a schematic diagram of the S1 layout and the twiss functions for the preliminary four-quadrupole optics. For this first optics test, the design rectangular common magnets were replaced with available sector dipoles. The strong quadrupole component of these magnets was compensated in the four Elytt quadrupoles. This optics does not constrain the value of r_{56} , which requires the full complement of eight quadrupole magnets.

The three sections of the vacuum system were welded, baked, installed and pumped down by the end of the first week in April. The support tables, S1 and FFAG magnets were surveyed into place to an accuracy of approximately 0.2 mm during this time as well. The cooling water manifolds and connections to the dipole magnets were pressurized on the evening of April 16. Operations began the following



Figure 4: View from upstream of the splitter S1 line and the Splitter and FFAG cell magnets for the Fractional Arc Test.

evening, when five of the six the linac cavities were initially calibrated and phased using time-of-flight measurements between beam position monitors at each end of the linac. With no linac acceleration, the gate valve to the S1 line was opened with the linac and the 6-MeV beam from the injector was visible on the view screen at the end of the S1 line. Each of the five cavities was then powered and the non-accelerating phase found by finding the beam on the view screen. The cavity phase was then moved 90 degrees, the S1 magnet settings scaled by the calibrated value of the summed accelerating gradients and finally fine-tuned to place the beam with sub-mm accuracy. These final adjustments were at the 0.2% level, testifying to the accuracy of the cavity calibrations and to that of the S1 dipole magnets, which had not yet been mapped. At a beam energy of 36 MeV, a spurious limit in the S1 magnet supply voltages was reached. The following evening, the procedure was repeated to achieve 42 MeV, the gate valve to the FFAG magnet array was opened, and the beam was observed on the view screen at the end of the F.A.T. line (see Fig. 7) following minor steering adjustments. The RMS size of the beam was 0.39 mm horizontally and 0.25 mm vertically, approximately round as expected.

SUMMARY

Initial commissioning of the first CBETA splitter/combiner line at 42 MeV has concluded. The design calibration of the dipole magnets was verified at the level of 0.2%. Four additional quadrupoles will be installed during the first week of May, enabling the implementation of the full design optics. This Fractional Arc Test will continue through May 18, providing detailed measurements of the field quality of the dipoles, quadrupoles and vertical correctors. Operation of CBETA with eight splitter/combiner lines and the full FFAG return loop will begin in early 2019.

Figure 5: Operating parameters of the S1 magnets for the 42-MeV electron beam

Type	S Position (m)	Length (m)	Momentum (MeV)	B field (T)	B integral (T-m)	Bd angle (degrees)	Bd Radius (m)	Sagitta (cm)	Gradient (T/m)	L (mH)	NI (kA-turns)	Power (V)	Supply (A)	Curr Density (A/mm ²)	
1 MD1DIP01	H-dip-4-A	22.473	0.100	6.000	0.0408	0.0052	0.000	0.000	0.000	230.00	0.592	1.4	1.7	0.33	
2 MS1DPB01	H-common	23.155	0.214	41.997	-0.3634	-0.0793	27.502	0.445	1.278	0.000	2.57	-4.469	-11.9	-223.5	-9.66
3 MS1DIP02	H-dip-1	24.483	0.160	41.997	0.2195	0.0440	-17.991	-0.509	-0.627	0.000	9.10	3.270	2.9	62.9	2.72
4 MS1DIP03	H-dip-1	25.368	0.160	41.997	-0.3805	-0.0763	31.226	0.294	1.083	0.000	9.10	-5.670	-5.0	-109.0	-4.72
5 MS1DIP04	H-dip-1	26.597	0.160	41.997	0.2839	0.0569	-23.262	-0.393	-0.810	0.000	9.10	4.231	3.7	81.4	3.52
6 MS1DIP05	H-dip-1	27.392	0.160	41.997	0.2839	0.0569	-23.262	-0.393	-0.810	0.000	9.10	4.231	3.7	81.4	3.52
7 MS1DIP06	H-dip-1	28.622	0.160	41.997	-0.3805	-0.0763	31.226	0.294	1.083	0.000	9.10	-5.670	-5.0	-109.0	-4.72
8 MS1DIP07	H-dip-1	29.505	0.160	41.997	0.2468	0.0495	-20.225	-0.453	-0.705	0.000	9.10	3.678	3.2	70.7	3.06
9 MS1DPB08	H-common	30.818	0.214	41.997	-0.3417	-0.0746	27.502	0.445	1.278	0.000	2.57	-4.203	-11.2	-210.1	-9.09
10 MS1QUA01	Quad-1-A	23.938	0.150	41.997	0.0000	0.0000	0.000	0.000	0.000	34.00	0.000	0.0	0.0	0.00	
11 MS1QUA02	Quad-1-A	24.909	0.150	41.997	0.0000	0.0000	0.000	0.000	0.000	34.00	0.000	0.0	0.0	0.00	
12 MS1QUA03	Quad-1-A	25.594	0.150	41.997	0.0000	0.0000	0.000	0.000	0.000	34.00	-0.248	-1.1	-3.0	-0.63	
13 MS1QUA04	Quad-1-A	26.312	0.150	41.997	0.0000	0.0000	0.000	0.000	1.799	34.00	0.365	1.7	4.4	0.93	
14 MS1QUA05	Quad-1-A	27.608	0.150	41.997	0.0000	0.0000	0.000	0.000	0.104	34.00	0.021	0.1	0.3	0.05	
15 MS1QUA06	Quad-1-A	28.326	0.150	41.997	0.0000	0.0000	0.000	0.000	-0.675	34.00	-0.137	-0.6	-1.7	-0.35	
16 MS1QUA07	Quad-1-A	29.010	0.150	41.997	0.0000	0.0000	0.000	0.000	0.000	34.00	0.000	0.0	0.0	0.00	
17 MS1QUA08	Quad-1-A	29.981	0.150	41.997	0.0000	0.0000	0.000	0.000	0.000	34.00	0.000	0.0	0.0	0.00	
18 MS1CRV01	V-cor-2	23.745	0.045	41.997	0.0000	0.0000	0.000	0.000	0.000	0.00	0.000	0.0	0.0	0.00	
19 MS1CRV02	V-cor-2	25.030	0.045	41.997	0.0000	0.0000	0.000	0.000	0.000	0.00	0.000	0.0	0.0	0.00	
20 MS1CRV03	V-cor-2	28.842	0.045	41.997	0.0000	0.0000	0.000	0.000	0.000	0.00	0.000	0.0	0.0	0.00	
21 MS1CRV04	V-cor-2	29.812	0.045	41.997	0.0000	0.0000	0.000	0.000	0.000	0.00	0.000	0.0	0.0	0.00	

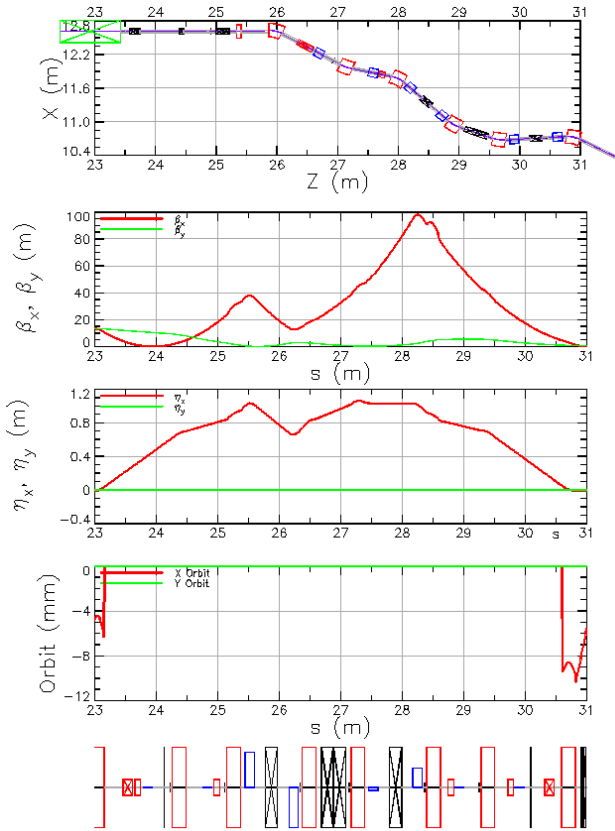


Figure 6: Twiss functions for the four-quadrupole S1 line optics.

ACKNOWLEDGMENTS

The authors wish to acknowledge important contributions from the technical and engineering staffs of Wilson Laboratory and the Brookhaven National Laboratory. This work is supported by NSF award DMR-0807731, DOE grant DE-AC02-76SF00515, and New York State Energy Research and Development Authority.

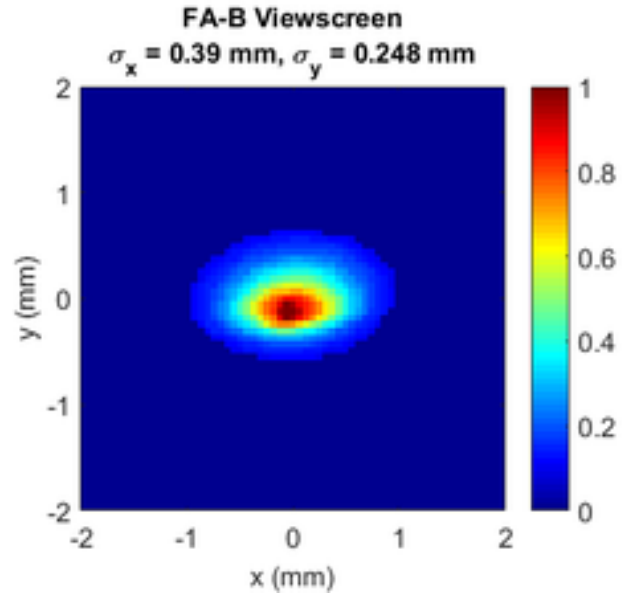


Figure 7: First 42-MeV beam spot observed at the end of the F.A.T. line.

REFERENCES

- [1] N. Banerjee *et al.*, “CBETA Design Report,” CBETA Technical Report CBETA-015, Cornell University and Brookhaven National Laboratory (2017).
- [2] G. Hoffstaetter *et al.*, “CBETA, the 4-Turn ERL with SRF and Single Return Loop,” (2018), TUYGBE2, these proceedings.
- [3] W. Lou *et al.*, “Front to End Simulations of the CBETA Energy Recovery Linac,” (2018), THPAF021, these proceedings.
- [4] W. Lou *et al.*, “Optical Design for the Cornell-Brookhaven Energy Recovery Linac Test Accelerator CBETA,” (2018), THPAF023, these proceedings.
- [5] J. Crittenden *et al.*, “Magnet Design for the Splitter/Combiner Regions of CBETA, the Cornell-Brookhaven Energy-Recovery-Linac Test Accelerator,” in *Proceedings of the 2016 North American Particle Accelerator Conference, October 9-14, 2016, Chicago, IL, USA* (2016).
- [6] R. Bass & J. Crittenden, “Comprehensive Tracking Study for the H-Dipoles and Common Magnets in the Splitter Sections

of the Cornell/Brookhaven Energy-Recovery-Linac Test Accelerator,” CBETA Technical Report CBETA-019, CLASSE, Cornell University (2017).

[7] “Elytt/Neureus Technologies, Madrid, Spain,” Orense 11, 28020 Madrid, Spain, <http://www.elytt.com>.